

# Experimental study on possible vortex shedding in a suspension bridge. Part II – Results when under typhoon Babs and York

S. S. Law<sup>†</sup>

*Civil and Structural Engineering Department, Hong Kong Polytechnic University,  
Hong Kong, People's Republic of China.*

Q. S. Yang<sup>‡</sup>

*Bridge Engineering Department, Beijing JiaoTung University, People's Republic of China.*

Y. L. Fang<sup>‡</sup>

*Mechanical Engineering Department, TaiYuen University, People's Republic of China.*

*(Received November 3, 2006, Accepted November 11, 2007)*

**Abstract:** Statistical analysis on the measured responses of a suspension bridge deck (Law, *et al.* 2007) show that vibration response at the first torsional mode of the structure has a significant increase at and beyond the critical wind speed for vortex shedding as noted in the wind tunnel tests on a sectional model. This paper further analyzes the measured responses of the structure when under typhoon conditions for any possible vortex shedding events. Parameters related to the lifting force in such a possible event and the vibration amplitudes are estimated with a single-degree-of-freedom model of the system. The spatial correlation of vortex shedding along the bridge span is also investigated. Possible vortex shedding events are found at both the first torsional and second vertical modes with the root-mean-square amplitudes comparable to those predicted from wind tunnel tests. Small negative stiffness due to wind effects is observed in isolated events that last for a short duration, but the aerodynamic damping exhibits either positive or negative values when the vertical angle of wind incidence is beyond  $\pm 10^\circ$ . Vibration of the bridge deck is highly correlated in the events at least in the middle one-third of the main span.

**Keywords:** wind; typhoon; dynamic; vortex shedding; suspension bridge; steel; traffic; model; optimization.

## 1. Introduction

Measured structural responses of a suspension bridge have been analyzed statistically in a companion paper (Law, *et al.* 2007), and vibration response at the first torsional mode of the

---

<sup>†</sup> Associate Professor, Corresponding Author, E-mail: [cesslaw@polyu.edu.hk](mailto:cesslaw@polyu.edu.hk)

<sup>‡</sup> Professor

structure was checked to have significant increase in the vibration magnitude at and beyond the critical wind speed for vortex shedding as noted in the wind tunnel tests on a sectional model. This paper analyses further the measured responses of the structure under typhoons BABS in 1998 and York in 1999. Parameters related to the lifting force in a possible vortex shedding event and the vibration amplitudes are estimated with a single-degree-of-freedom model of the system.

There is no full-scale pressure or wake measurement on the structure to confirm the existence of vortex shedding. This study infers the presence of vortex shedding through the response measurements by monitoring the structural motions. Initial criteria for a possible vortex shedding event will be given, and any evidence that is supportive to the definition of a vortex shedding event will be highlighted in the development of this study.

## 2. The permanent instrumentation systems

A Structural Health Monitoring System (SHMS) has been installed on the bridge structure. Wind conditions and acceleration responses of the structures are some of the information collected by the system. There are six anemometers and 24 uni-axial servo type accelerometers on the structure. Two digital ultrasonic anemometers (Gill Wind Master Ultrasonic anemometer) were installed on both the north edge and south edge of the bridge deck at midspan (Section *I*). They are specified as WITJN01 and WITJS01 in Figs. 1 and 2. Each ultrasonic anemometer can measure three components of wind velocity simultaneously. Two analogue mechanical anemometers were located at the two edges of the bridge deck near the middle of the West side span (Section *C*), specified as WITBN01 at the north side and WITBS01 at the south side as shown in Figs. 1 and 2. Each analogue mechanical anemometer consists of a horizontal component of model RM YOUNG 05106 Horizontal Anemometer, and a vertical component of model RM YOUNG 27106 Vertical Anemometer. Both of them measure the wind velocity only. Another two analogue mechanical anemometers of horizontal component only were installed at a level 11m above the top of the two bridge towers (Sections *E* and *K*). They are specified as WITPT01 for the East tower and WITET01 for the West tower as shown in Fig. 2.

The servo accelerometers are of model Allied Signal Aerospace Q-Flex QA700. Three different types of arrangement for acceleration measurement were used in the system, namely AccT, AccB and AccU as indicated in Fig. 2, representing the Tri-axial measurement, Bi-axial measurement and Uni-axial measurement respectively. A total of twelve uni-axial accelerometers were located on

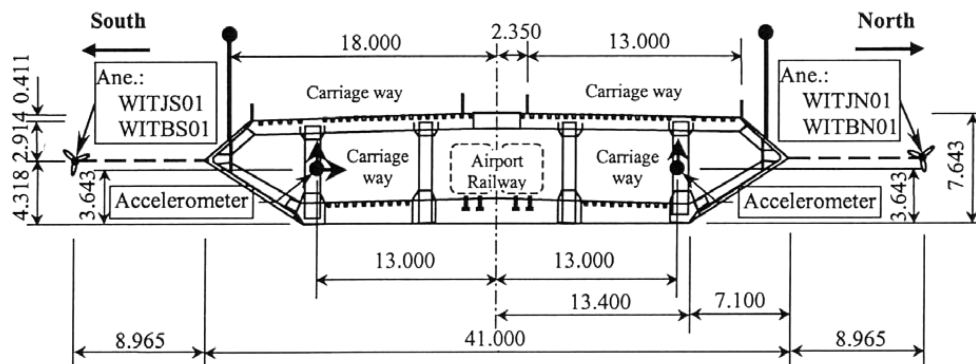


Fig. 1 Cross-section of bridge deck and sensor locations (dimensions in metre)

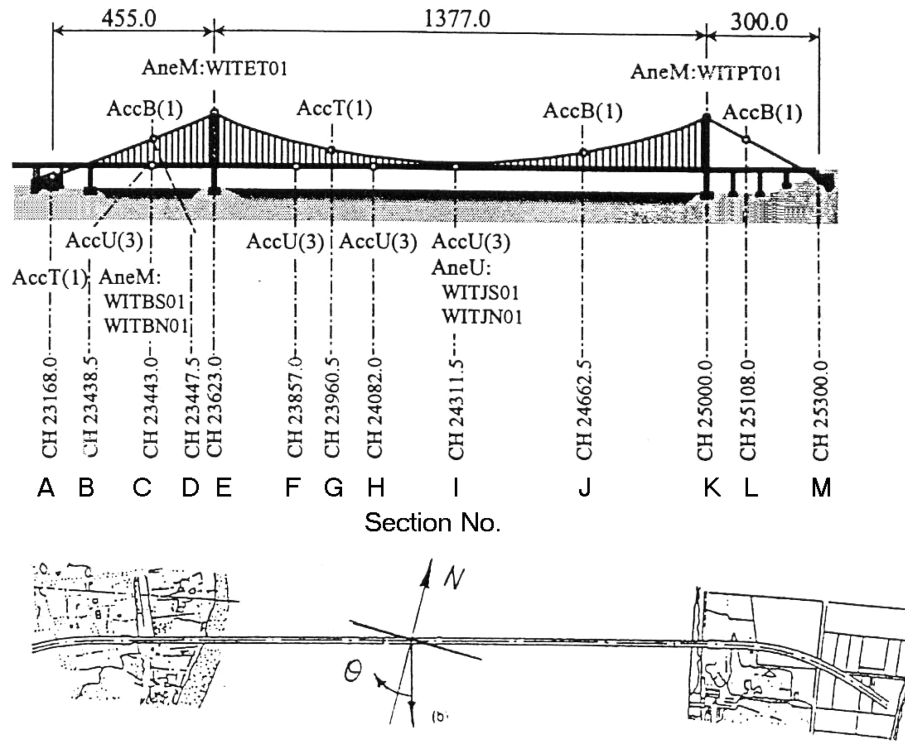


Fig. 2 Location of instruments (dimensions in metre)

Sections *B*, *F*, *H* and *I* of the bridge deck as shown in Fig. 2. They are at the end pier of West side span, one-sixth span, one-third span and half-span length of the main span of the bridge deck respectively. At each of these sections, there are two accelerometers measuring acceleration in the vertical direction spaced 26.8 metres apart, and one accelerometer measuring acceleration in the lateral direction as shown in Fig. 1. The sampling frequencies are 2.56Hz and 25.6Hz for recording the wind data and acceleration responses, respectively.

### 3. The second experimental study

The second study analyses the data collected in two periods of measurement. The first period starts from 20:00 on 20 February 1998 to 24:00 on 21 February 1998. It consists of two segments of data with a total duration of 26 hours. The second period starts from 06:00 on 25 October 1998 to 23:00 on 26 October 1998. It consists of 41 hours of data. The first period coincides with strong seasonal wind from the north, and the second period coincides with the passage of typhoon BABS over Hong Kong when typhoon signal No. 3 was up. Normal traffic condition was maintained throughout these two periods.

#### 3.1. Data analysis

The structural response at Section *I* (midspan of main span) from the first period were inspected for any possible vortex shedding events at the second vertical mode, while those from the second

period were inspected for events at the first torsional mode. Section *I* corresponds to the location where the second vertical and first torsional mode shapes have the largest responses. The vertical acceleration is taken as the average of the readings from the two vertical sensors in the cross-section, while the torsional acceleration is obtained as half of the difference of the readings of the vertical sensors. The three components of the wind velocity obtained from the anemometer WITJN01 at midspan of the bridge deck are processed. Those from WITJS01 at the same cross-section are corrupted and cannot be used.

### 3.2. Wind characteristics

The one-minute moving averages of the following wind characteristics were computed: the horizontal incident wind speed, the turbulence intensity, horizontal and vertical incident angle, and the vertical wind speed. The first four parameters were plotted in Figs. 3 and 4 for the two time periods under study. The horizontal angle starts from the normal line on the south edge of the deck and rotates clockwise as shown in Fig. 2. In the first period of 28 hours, the incident wind speed increased from approximately 2 m/s at the beginning to 7 m/s after 14 hours while large variations existed in the latter half of the time history. The horizontal wind angle varied from  $290^\circ$  to  $360^\circ$  in the first half of the time period. It also varied greatly in the latter half of the time history which corresponded to the passage of Typhoon BABS. The turbulence intensity is less than 0.2 in general. The vertical angle of incidence varied between  $\pm 10^\circ$  most of the time, and the vertical wind speed varied between  $\pm 2$  m/s and is not shown.

In the second time period, the incident wind speed is above 10 m/s most of the time, and it sometimes goes above 16 m/s. The turbulence intensity plot shows fairly stable values below 0.2 except some high values near the beginning and end of the time period. The horizontal incident wind angle is approximately at  $30^\circ$  ( $13.4^\circ$  from the normal line) for the first 19 hours with large variation in the latter part of the time period. Typhoon BABS was closest at a point 240 km South-East-East of Hong Kong at 08:00 on 26 October 1998. Maximum hourly wind speed and maximum gust measured by the Hong Kong Observatory at Waglan Island are 22.5 m/s and 31.4 m/s respectively. The vertical angle of incidence varied between  $\pm 10^\circ$  with larger variation at the beginning and end of the period. The vertical wind speed varied between  $\pm 2$  m/s for the whole period and is not shown.

### 3.3. Structural responses

The acceleration signals are filtered to remove the close to DC components of the signal. They are then integrated to obtain the velocity and displacement signals by using a proven time integration algorithm (Petrovski and Naumovski 1979) with a maximum error of 1.2% maintained in the integrated results.

Response of a vortex shedding event is narrowband as compared to the buffeting response which encompasses a much wider bandwidth response, but both of them are responses under forced excitations. Therefore possible vortex shedding events are sought with the following two criteria: (a) there is only a major spectral peak in the power spectral density function (PSD) at the natural frequency of interest, and the ratio of any secondary frequency PSD component to the main PSD component is less than 0.05; and (b) the phase diagram plotting the velocity against displacement should approach a circular shape indicating force excitation with a close to  $90^\circ$  phase difference.

The vibration modes of the structure are distinct (Law, *et al.* 2007) and any modal coupling effect



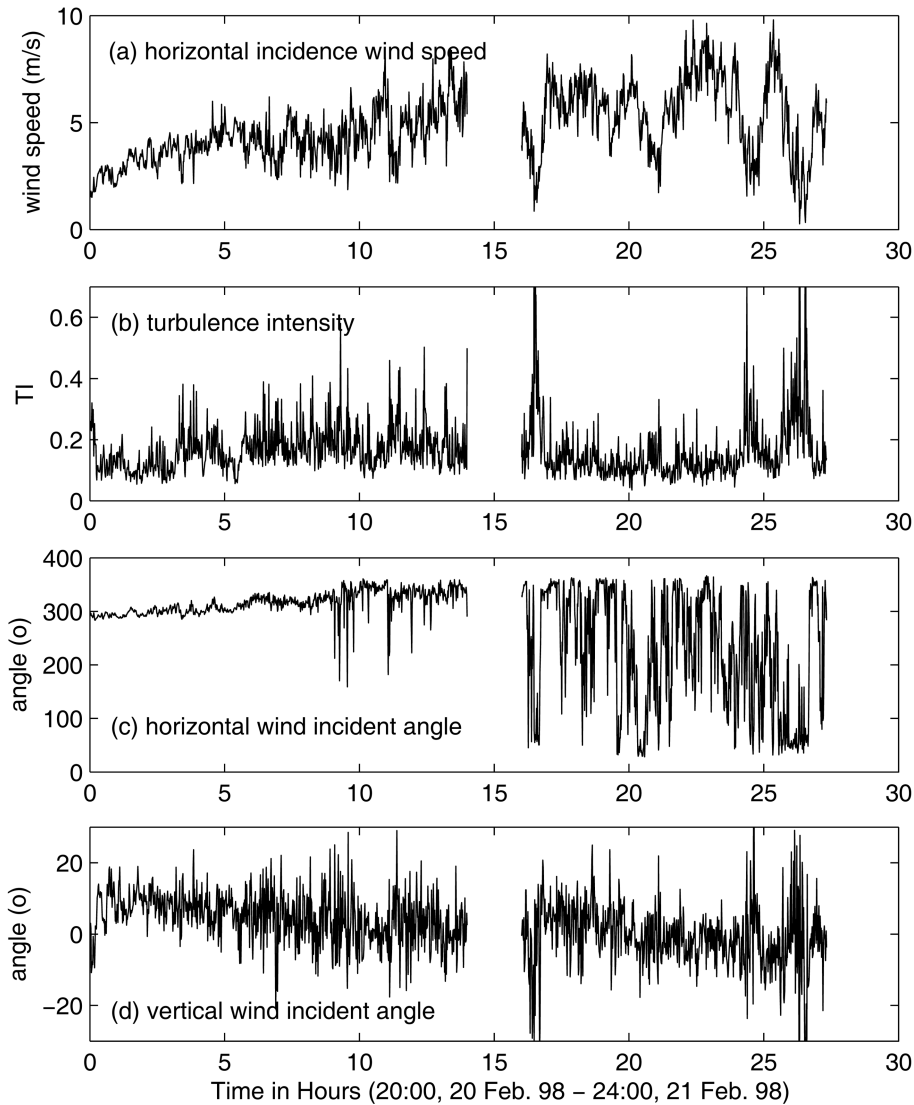


Fig. 3 One minute average wind characteristics (Feb. 1998)

is assumed insignificant. The time response data was inspected and segments of data with a minimum of 6 cycles and 5 cycles of the responses satisfying the above criteria, which correspond to 43.2s and 18.7s for the second vertical and first torsional modes respectively in the time histories, were analysed to estimate the parameters. 80 and 226 possible events were identified associated with the second vertical and first torsional modes respectively. Most of the events for the second vertical mode occurred between 12:00 and 22:00 on 21 February 1998, and those for the first torsional mode occurred between 16:00 25 October and 01:00 26 October 1998. Fig. 5(a) shows the time history of a typical forced excitation response found at the second vertical mode. The energy input into the structure from wind varies with the wind speed. The forced response may occur again before the last one decays to the normal vibration level. Fig. 5(b) shows such an event with changes

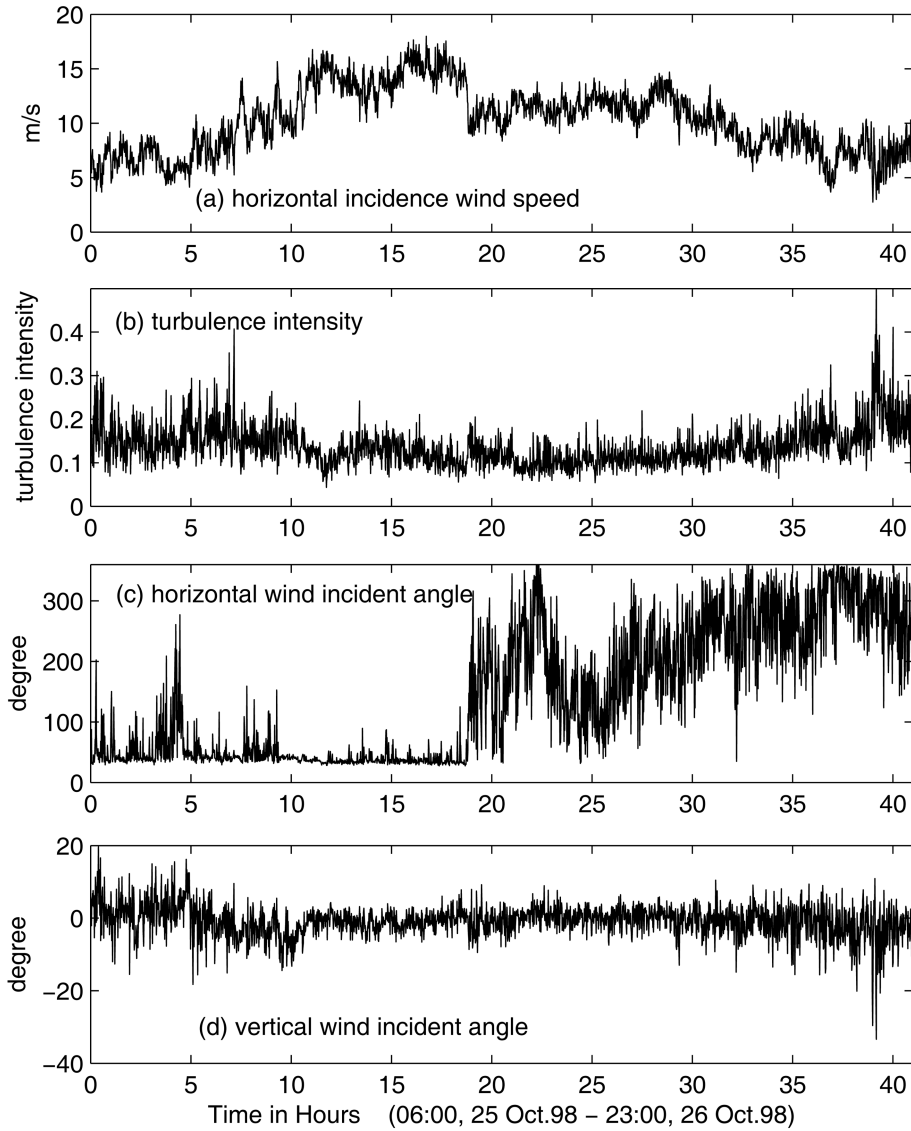


Fig. 4 One minute average wind characteristics (Oct. 1998)

in the energy input from wind. It is noted from the envelope of the time histories that the wind excitation does not remain constant for a long time. A time period with a response close to harmonic oscillation is extracted from Fig. 5(a) and processed, and Fig. 6 shows the time history, the PSD and the normalized phase diagram. This time period is noted to satisfy the two criteria for a possible vortex shedding as stated earlier.

### 3.4. Analysis results

The horizontal and vertical incidence wind angle, the turbulence intensity, the average wind speed and the RMS amplitude of vibration of the bridge deck are computed for all the identified time

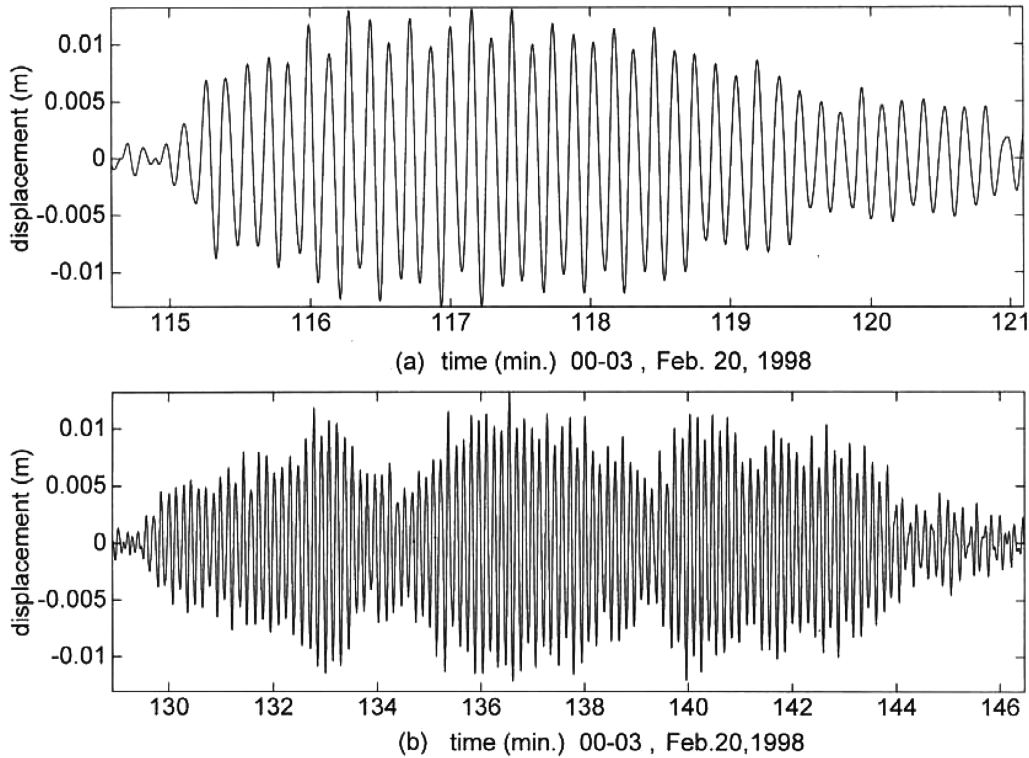


Fig. 5 Sample of forced response events at the second vertical mode  
(a) single event; (b) multiple events

periods. The SDOF model is fitted to each of these events, and the damping and stiffness parameters  $I_1$  to  $I_4$  are computed using Eqs. (7) to (15) in the companion paper (Law, *et al.* 2007) with a measured damping ratio of 0.02, and they are plotted in Figs. 7 and 8 together with the turbulence intensity and the RMS values for the second vertical and first torsional modes respectively. The graphs are plotted as scatter diagram with the wind speed in the horizontal axis, and the vortex shedding events are categorized into five groups according to the vertical incidence angle with the following notations: o denotes those between  $-10^\circ$  and  $-5^\circ$ ; + denotes those between  $-5^\circ$  to  $0^\circ$ ; × denotes those between  $0^\circ$  and  $+5^\circ$ ; \* denotes those between  $+5^\circ$  and  $+10^\circ$ ; and ⊗ denotes those above  $+10^\circ$  or below  $-10^\circ$ .

The RMS plots show the vibration amplitude increases parabolically with wind speed with large amplitudes of vibration at a wind speed between 5.8 to 7.6 m/s and between 12.4 and 16.1 m/s for the second vertical and first torsional modes respectively. If the measured natural frequencies are adopted and a Strouhal number of 0.155 is used, the critical wind speed would be 6.8 m/s and 13.1 m/s for the second vertical and first torsional modes respectively, and they are within the speed ranges identified in the wind tunnel tests. The turbulence intensity computed for the vortex shedding events is within the range of 0.05 to 0.15 over these ranges of wind speed for the two modes. Parameters  $I_2$  and  $I_3$  are zero at the critical speed and their influences may be neglected. Indices  $I_1$  and  $I_4$  have negative values over the range of wind speed identified above. The range of parameters at the critical speed is noted and they are listed in Table 1 for discussions later.

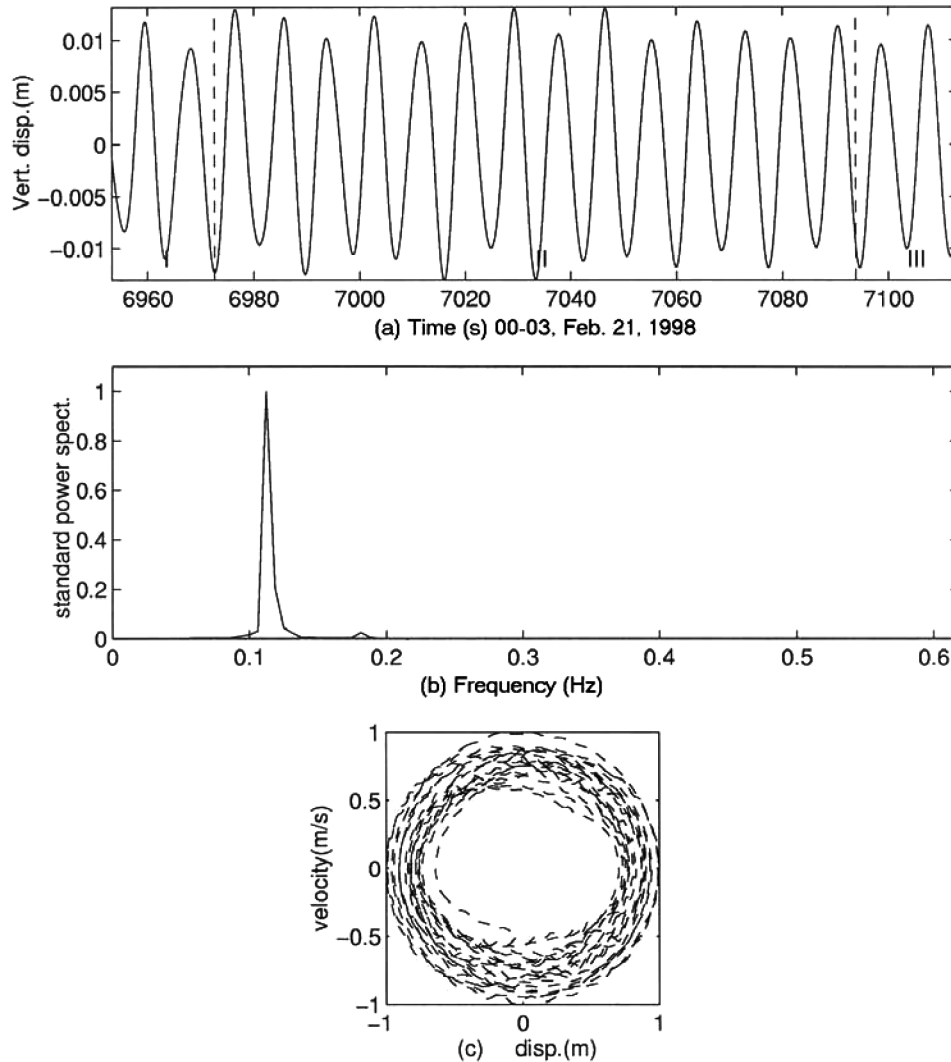


Fig. 6 Criteria of acceptance of a vortex shedding event  
(a) time history; (b) power spectrum; (c) phase diagram

The RMS plot of the vibration amplitude shows that the vertical incident angle has little relation to the vibration with large amplitudes for the second vertical mode as shown in Fig. 7(a). But the vertical incident angle does have an effect on the deck vibration at the first torsional mode. Most of the events with large amplitude occurred with a vertical incident angle between  $+5^\circ$  and  $-5^\circ$ , and those with a negative angle would give much larger amplitude of vibration than those with a positive angle. This observation is different from that made in the wind tunnel tests where the bridge deck has a smaller amplitude of vibration at negative angle of incidence.

Specific events with the RMS value exceeding 10 mm and 200 mm for the second bending and first torsional modes respectively are extracted and they are shown in Table 2. There are six such events in the second vertical mode. The vortex capture wind speed is between 5.8 to 8.6 m/s with a

Table 1 Summary of parameters identified in vortex shedding events at different sections

Section	Critical Wind speed ( $U$ )	RMS value (mm)	Horizontal Incident angle	Turbulence intensity	Vertical Incident Angle	Parameters				$\frac{UI_1}{2\zeta\omega_n}$	$\frac{U^2 I_4}{2\omega_n^2}$
						$I_1$	$I_2$	$I_3$	$I_4$		
20~21 Feb. 1998 (Second vertical mode- with normal traffic and trains) (refers to Table 2(a))											
$I$	$\approx 7.6$ m/s	<15	4 <sup>th</sup> quadrant (290°~360°)	<0.15	-5°~+5°, >+10°, <-10°	-0.05	0.0	0.0	-0.004	-10.9	-0.15
						~ -0.02			~ 0.0	~ -4.4	~ 0.0
25~26 Oct. 1998 (First torsional mode- with normal traffic and trains) (refers to Table 2(b))											
$I$	$\approx 14$ m/s	<335	1 <sup>st</sup> quadrant ( $\approx 30^\circ$ )	<0.15	-5°~+5°	-0.12	0.0	0.0	-0.004	-25.0	-0.14
						~ -0.02			~ 0.0	~ -4.2	~ 0.0
16 Sept. 1999 (First torsional mode- without traffic and trains)											
$I$		<400		<0.2		-0.09	-35000	-1.5E+10	-0.007	-21.5	-0.32
						~ +0.05	~ +38000	~ +1.7E+10	~ +0.001	~ +11.9	~ +0.045
$H$		<300	3 <sup>rd</sup> quadrant ( $\approx 220^\circ$ )	<0.3		-0.09	-50000	-1.7E+10	-0.0095	-21.5	-0.43
						~ +0.1	~ +55000	~ +9.0E+9	~ 0.0	~ +23.8	~ 0.0
			to		>+10° <-10°	-0.045	-1.8E+5	-8.0E+10	-0.0022	-10.7	-0.10
						~ +0.03	~ +1.0E+5	~ +2.0E+10	~ 0.0	~ +7.2	~ 0.0
$F$	$\approx 16$ m/s	<120	4 <sup>th</sup> quadrant ( $\approx 310^\circ$ )	<0.3		-0.04	-1.3E+6	-8.0E+12	-0.005	-9.5	-0.23
						~ +0.04	~ +1.7E+6	~ 1.7E+13	~ +0.001	~ +9.5	~ +0.045
$B$		<36		<0.25		-0.04	-1.3E+6	-8.0E+12	-0.005	-9.5	-0.23
						~ +0.04	~ +1.7E+6	~ 1.7E+13	~ +0.001	~ +9.5	~ +0.045

Note: (\*) indicates approximate average horizontal angle of wind

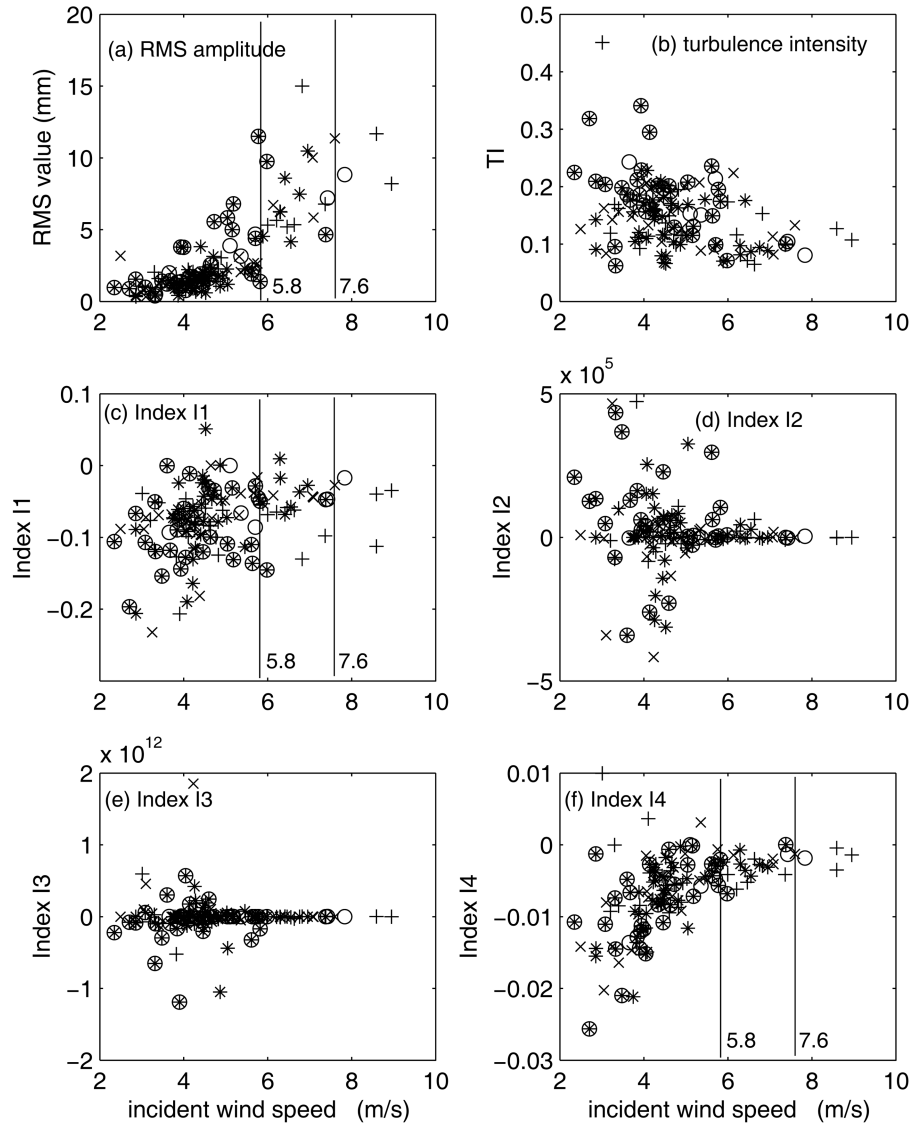


Fig. 7 Parameters of forced excitation responses at second vertical mode (Feb. 1998)

RMS value between 10 to 15 mm. The vertical angle of incidence is within  $\pm 5^\circ$  except the third one with a large positive angle of  $21^\circ$ . The turbulence intensity is quite high around 0.15. The mean wind speed is 7.6 m/s and the mean parameters  $I_1$  and  $I_4$  are respectively  $-0.06348$  and  $-0.0022$ . It is noted that a positive  $I_4$  would indicate a reduced stiffness of the system in a vortex shedding event. These values compare favorably with those from the wind tunnel tests (Table 2. of the companion paper) where the vortex capture velocity is between 6.9 to 9.4 m/s.

There are 18 events in the first torsional mode. The vortex capture wind speed is between 11.1 to 16.3 m/s with a RMS amplitude between 200 to 335 mm at the edge of the bridge deck. The vertical angle of incidence is within  $\pm 5^\circ$  with many negative values. The turbulence intensity is smaller than 0.16. The mean wind velocity is 14 m/s and the mean parameters  $I_1$  and  $I_4$  are

Table 2(a) Vortex shedding events in second bending mode at Sections *H* and *I*

Event No.	Duration (sec.)	RMS amplitude (mm)	Wind Speed (m/s)	Turbulence intensity	Horizontal incidence angle (°)	Vertical incident angle (°)	Index $I_1$	Index $I_4$
1	50.8	15.0 (7.25)	6.8	0.15	233.3	-4.3	-0.13024 (-0.14508)	-0.00292 (-0.00308)
2	50.8	11.7 (5.9)	8.6	0.13	221.8	-3.9	-0.03985 (-0.03578)	-0.00044 (-0.00030)
3	46.9	11.5	5.8	0.19	343.2	21.0	-0.04520	-0.00565
4	78.2	11.4 (6.8)	7.6	0.13	159.1	1.1	-0.02732 (-0.03336)	-0.00128 (-0.00191)
5	58.7	10.5 (6.2)	7.0	0.09	337.2	5.6	-0.02768 (-0.05038)	-0.00313 (-0.00370)
6	58.7	10.0	7.1	0.11	327.3	4.5	-0.04317	-0.00192
Mean		7.6 (7.5)					-0.06348 (-0.06615)	-0.0022 (-0.002248)

Note: (\*) indicates values obtained at Section *H*.Table 2(b) Vortex shedding events in first torsional mode at Sections *H* and *I*

Event No.	Duration (sec.)	RMS amplitude (mm)	Wind speed (m/s)	Turbulence intensity	Horizontal incidence angle (°)	Vertical incident angle (°)	Index $I_1$	Index $I_4$
1	46.9	334.2	12.7	0.13	35.2	-4.5	-0.01091	-0.00155
2	27.4	299.6 (241.3)	14.0	0.09	34.2	-2.8	-0.01975 (-0.01535)	-0.00274 (-0.00260)
3	35.2	267.9	11.1	0.16	40.0	-6.4	0.06314	-0.00354
4	23.5	261.4 (218.2)	16.3	0.09	87.7	-5.1	-0.03591 (-0.09484)	-0.00163 (-0.00137)
5	23.5	261.3	11.3	0.13	41.1	2.7	0.09743	-0.00021
6	35.2	251.0	15.5	0.08	31.9	-3.0	-0.03006	-0.00179
7	23.5	243.2	13.5	0.12	40.3	-0.2	-0.06278	0.00109
8	35.2	238.7	14.4	0.12	40.1	-1.5	-0.02624	-0.00129
9	39.1	235.5 (194.9)	13.5	0.13	43.6	-1.5	-0.07782 (-0.09458)	-0.00070 (-0.00062)
10	27.4	224.9	14.9	0.09	25.8	-3.0	-0.05435	-0.00253
11	27.4	223.2 (198.6)	12.3	0.10	37.6	-0.9	-0.01230 (-0.03895)	-0.00292 (-0.00082)
12	35.2	222.8	15.4	0.14	27.9	-5.1	-0.05299	-0.00177
13	27.4	220.5 (175.0)	14.2	0.15	30.1	-3.4	-0.02265 (-0.00548)	-0.00204 (-0.00238)
14	23.5	216.1	14.4	0.13	46.7	-5.0	-0.08977	-0.00176
15	27.4	208.9 (168.4)	13.0	0.11	34.3	3.6	-0.03887 (-0.04113)	-0.00233 (-0.00321)
16	35.2	203.6 (171.4)	14.8	0.13	37.9	0.9	-0.03459 (-0.02397)	-0.00088 (-0.00022)
17	39.1	203.2	13.0	0.09	36.0	-2.6	-0.02511	-0.00301
18	23.5	200.2	14.7	0.13	36.4	-4.1	-0.02556	-0.00308
Mean			14.0 (14.4)	-	-	-	-0.025505 (-0.0449)	-0.00187 (-0.0016)

Note: (\*) indicates values obtained at Section *H*.

respectively  $-0.0255$  and  $-0.00187$ . The range of wind speed also compares favorably with those from the wind tunnel tests (Table 2 of the companion paper) from 15.0 to 19.9 m/s for different angle of incidence.

### 3.5. Spatial correlation analysis of response

Since there is no information on the wind direction from the anemometer at Section C at midspan of West side span, study on the spatial correlations in the forced response event can only be done through comparison of the parameters in each event along the structure, i.e., the RMS amplitude

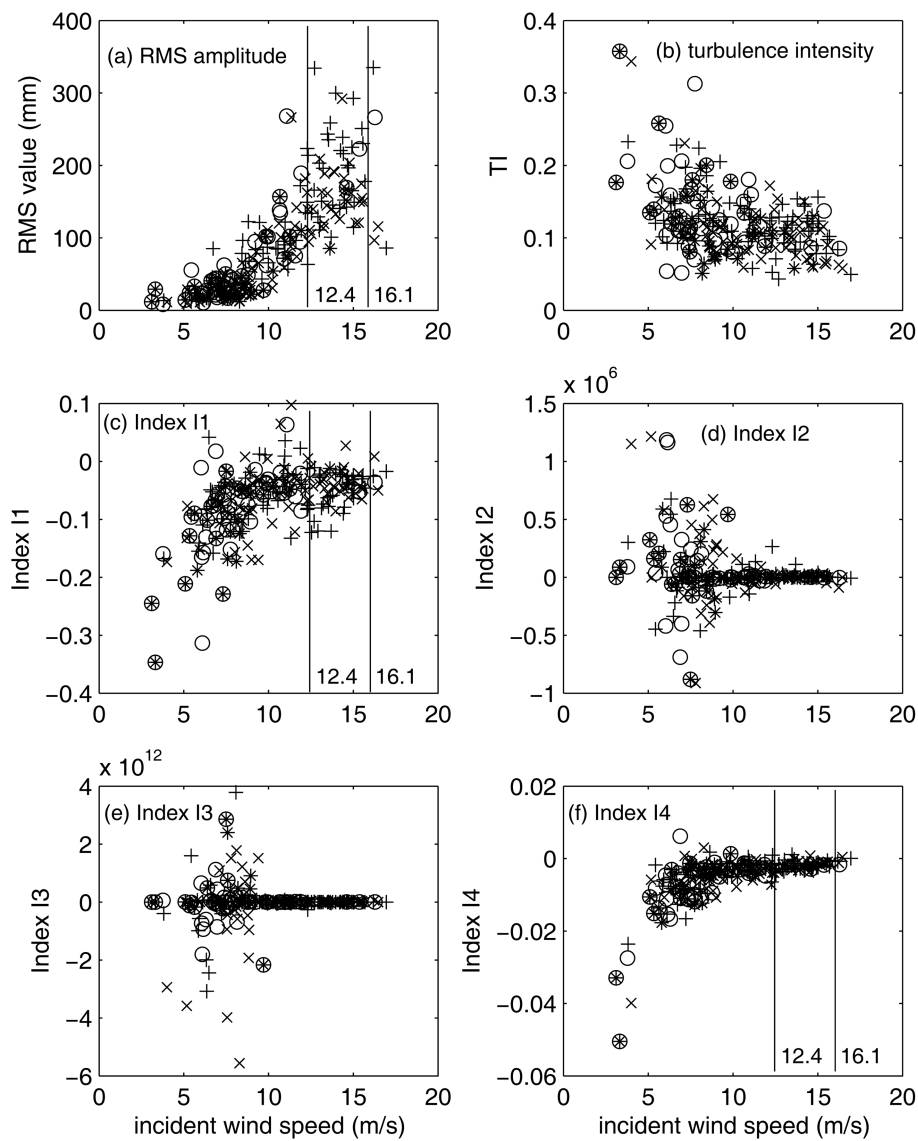


Fig. 8 Parameters of forced excitation responses at first torsional mode (Oct. 1998)



and the lift force coefficients at different cross-sections of the bridge deck. The acceleration responses collected at section *H* (one-third span of the main span) is again inspected, and forced response events at the second vertical and first torsional modes were found in several of the time periods shown in Table 2 at Section *I*. There are four and seven such events at the second vertical and first torsional modes respectively at Section *H*, details of them are presented in Table 2. Parameters  $I_2$  and  $I_3$  are close to zero in these periods. The averages of the indices  $I_1$  and  $I_4$  are almost the same as those in Section *I* for the second vertical mode. The value of  $I_4$  is similar to that found in section *I* for the first torsional mode. But  $I_1$  takes up an average value of  $-0.0449$  which almost doubles that found at Section *I*. This means a larger aerodynamic damping exists at Section *H* than at Section *I*.

### 3.6. Summary on the parameter estimation

Possible vortex shedding events are identified satisfying the criteria for a SDOF vibration system under forced excitation close to the critical wind speed. Parameters relating to the aerodynamic stiffness and damping coefficients are estimated with the Christensen's model.

The linear damping and stiffness parameters  $I_1$  and  $I_4$  are negative providing additional stability to the structure. The value of  $I_4$  is very small indicating an insignificant wind effect on the overall stiffness of the system. The non-linear damping parameters  $I_2$  and  $I_3$  are close to zero. There is also evidence indicating that aerodynamic damping at Section *H* is larger than that at Section *I* for the first torsional mode.

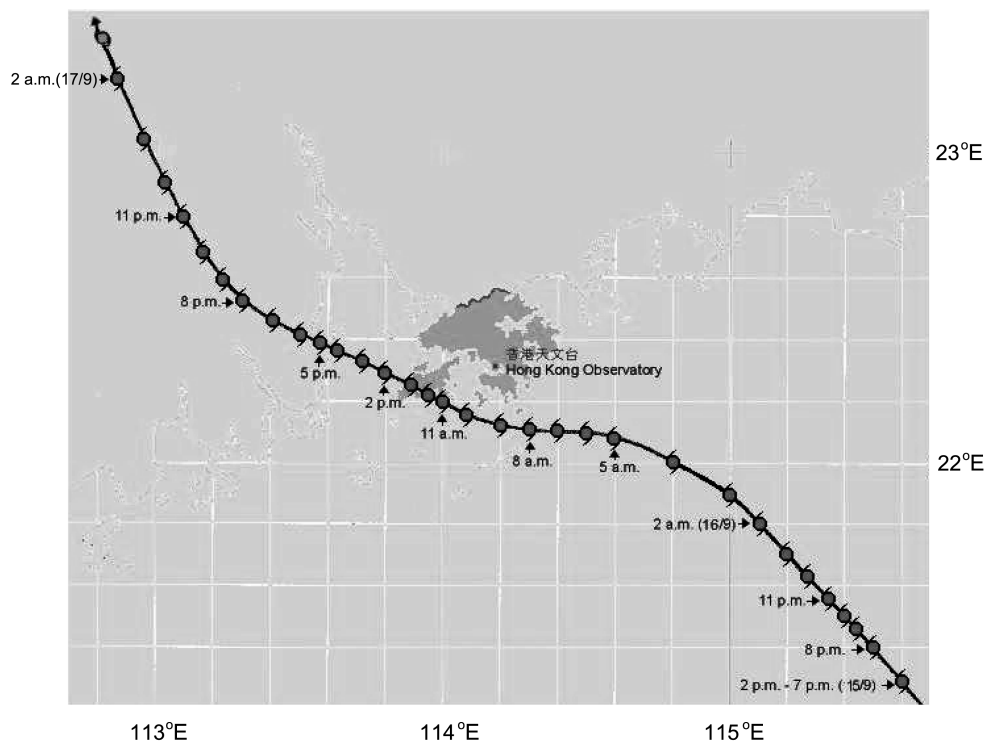


Fig. 9 Track of typhoon YORK passing through Hong Kong

#### 4. The third experimental study

The third study makes use of the wind and acceleration data collected on the bridge during the passage of typhoon YORK over Hong Kong. It covers a period from 00:00 to 20:00 on 16 September 1999 during which normal traffic and trains were forbidden on the bridge deck.

##### 4.1. Wind characteristics

Typhoon YORK was the strongest typhoon visited Hong Kong since 1983 and typhoon signal No. 10 was up for more than 11 hours. The track of the typhoon relative to Hong Kong is shown in Fig.

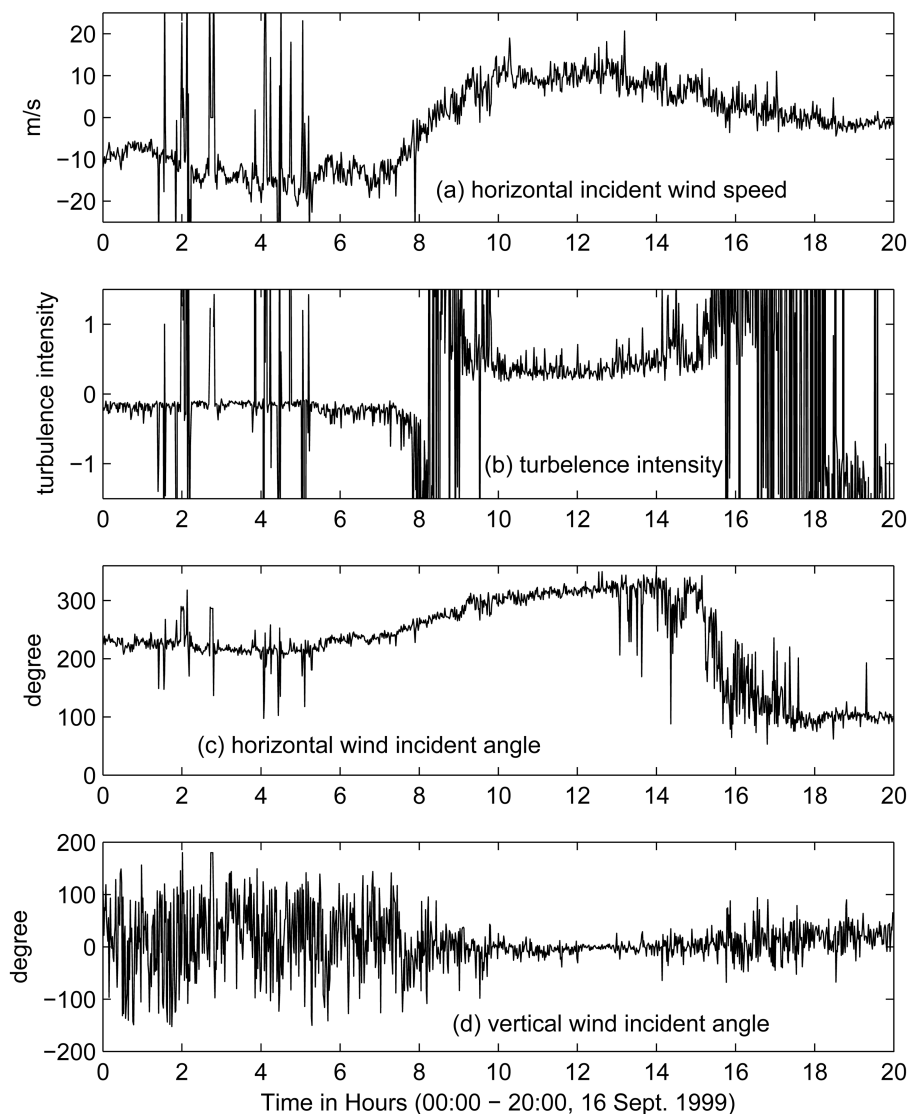


Fig. 10 One minute average wind characteristics (Sept. 1999)

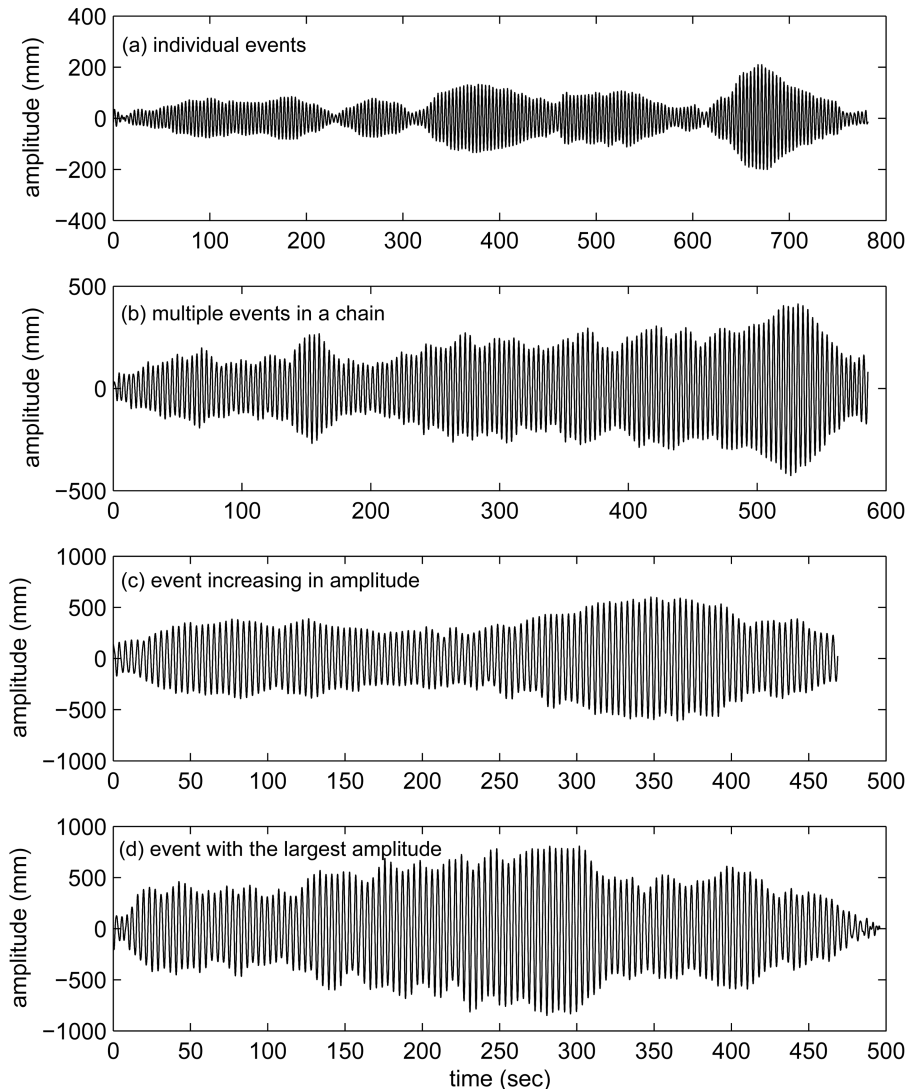


Fig. 11 Samples of possible vortex shedding at the first torsional mode (Sept. 1999)

9. It was within 20 km to the southwest of the bridge at its closest point at about 11:00. The Hong Kong Observatory recorded a maximum hourly wind speed of 42 m/s.

The wind data from the ultrasonic anemometer WITJN01 on the north edge of the bridge deck at Section I (midspan) are extracted. The one-minute moving averages of the horizontal incident wind speed, the turbulence intensity, horizontal and vertical angle of incident are calculated and plotted in Fig. 10. The very large incident wind speeds shown between 01:00 to 06:00 is due to mal-function of the equipment leading to erroneous turbulence intensity as shown. The large turbulence intensity occurrences observed in the rest of the time duration are correct. The wind takes up an average incident angle of  $220^\circ$  ( $23.4^\circ$  to the normal line) when approaching Hong Kong, and  $310^\circ$  ( $66.6^\circ$  to the normal line) when leaving Hong Kong. The wind is almost parallel to the bridge deck in the

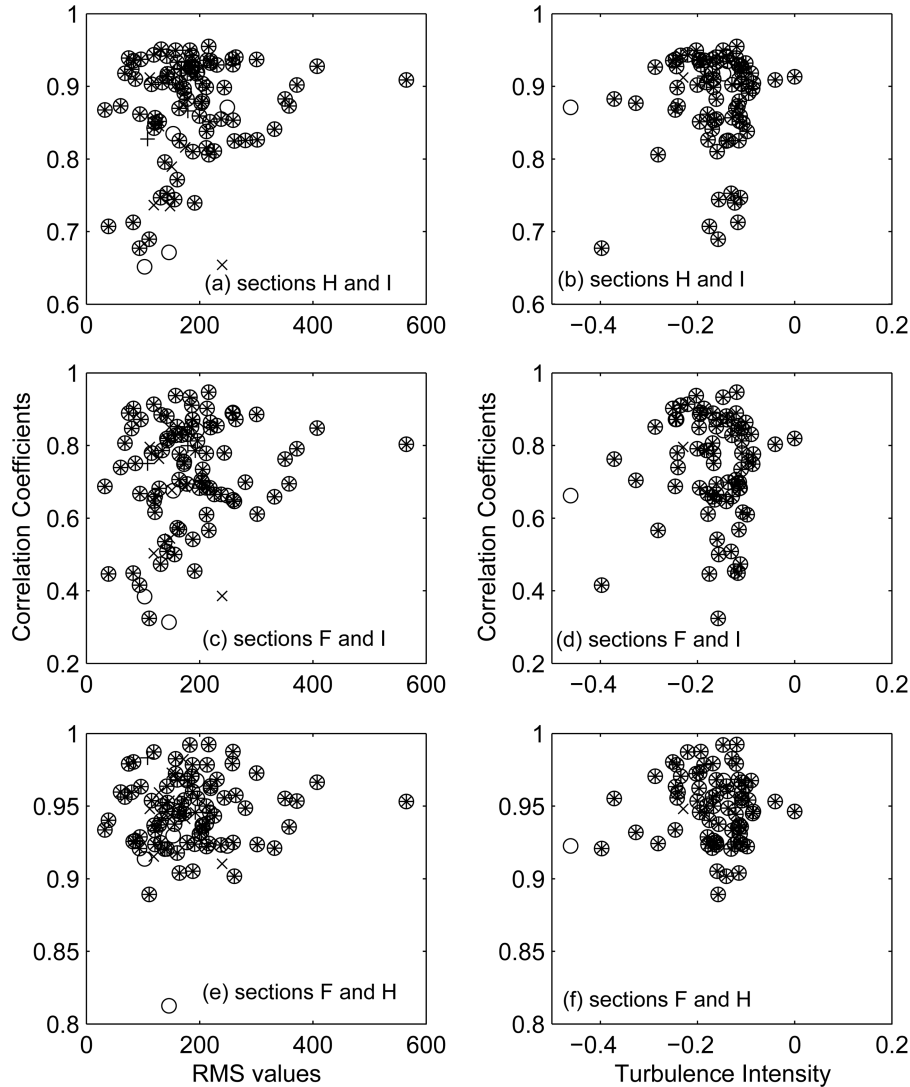


Fig. 12 Correlation between vibration at different sections of deck

latter case, and it corresponds to a very steady and small vertical incident angle as shown.

#### 4.2. Structural responses

Since the first torsional mode has been identified to have significant vibration under wind in the Second Study, this Study focuses on this type of vibration under typhoon York. The same technique as for the Second Study was applied to analyze the structural responses of the bridge deck. There are 41, 32, 63 and 96 possible events identified for the first torsional modes at Sections *B*, *F*, *H* and *I* respectively. Those for the other vibration modes have not been studied. Most of the time periods are between 00:00 to 09:00 and between 13:00 to 18:00. These time periods have been checked to correspond to good wind speed data. The forced vibration response events occurred in the early

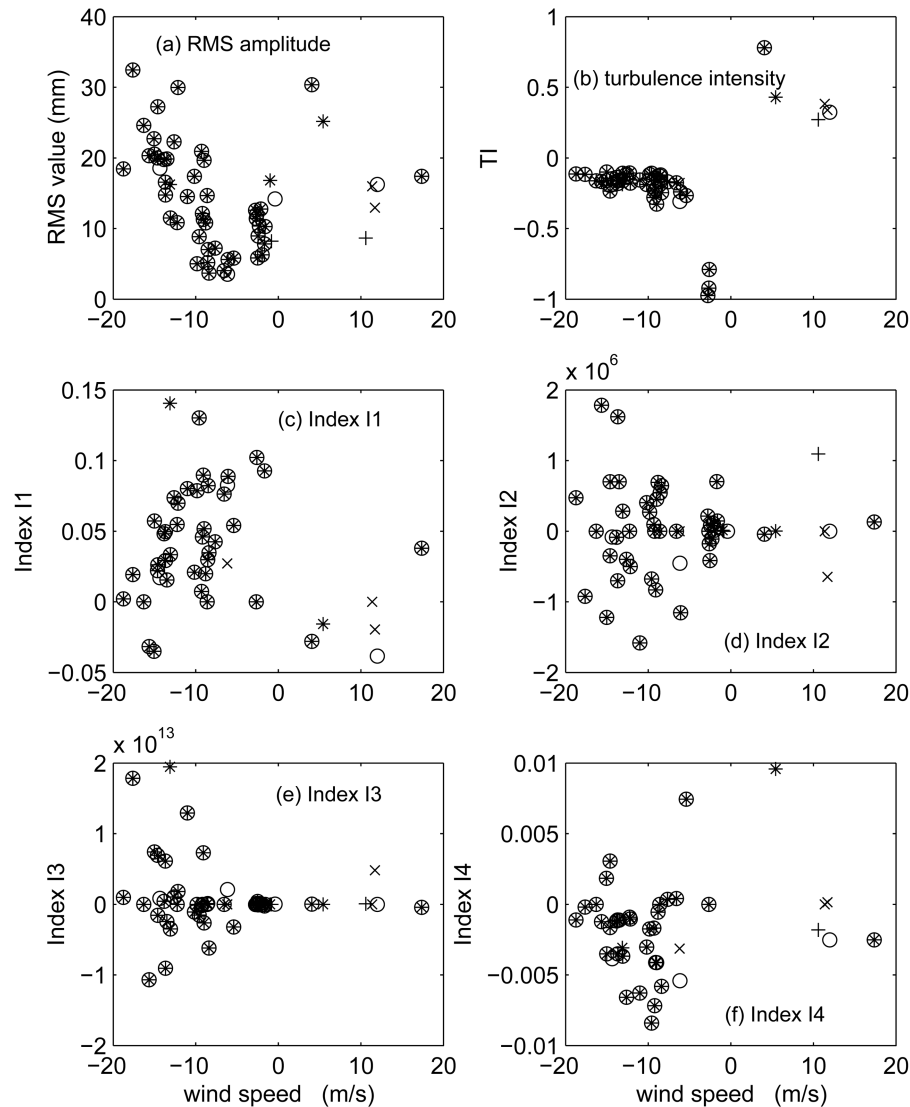
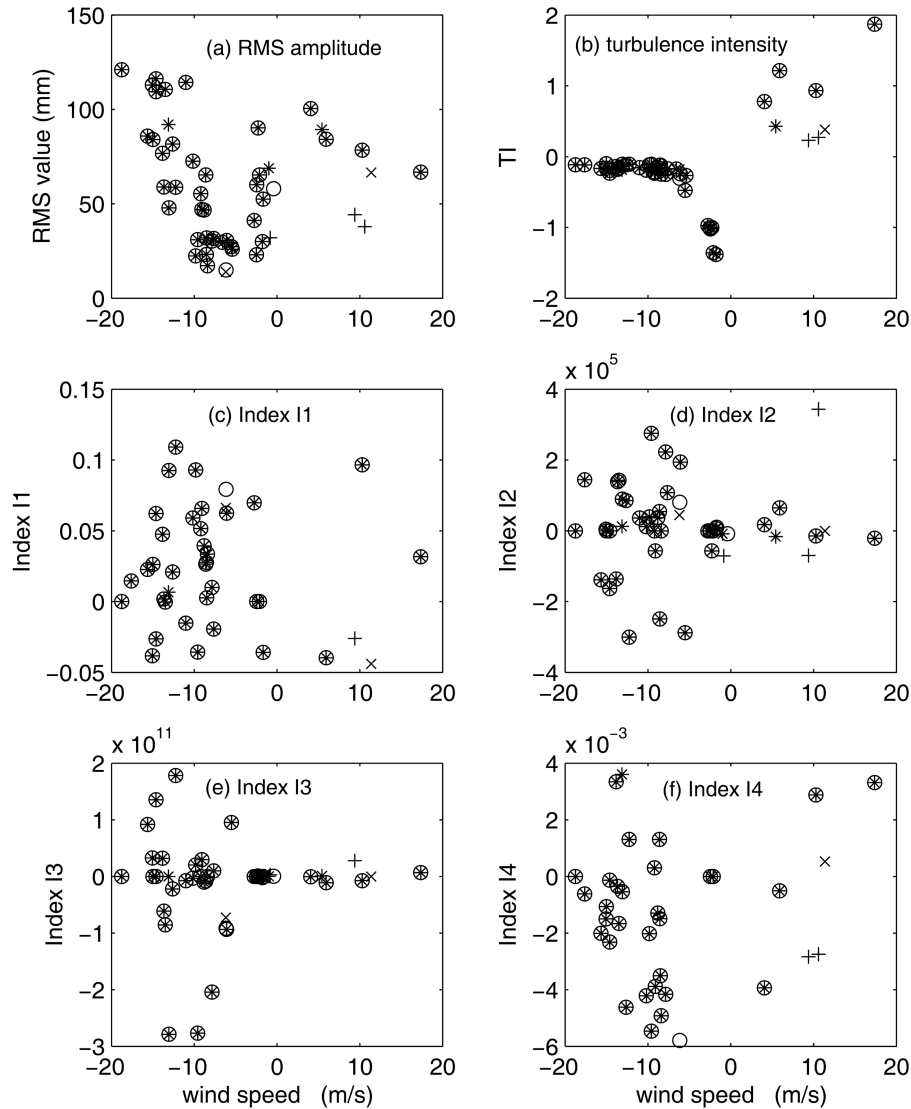


Fig. 13 Parameters of forced excitation response at Section B at first torsional mode (Sept. 1999)

morning are single events with approximately 100 seconds duration. When the wind speed increases, several of them occurred in connected sequence with 400 to 500 second duration. The event chain grew in amplitude with increasing wind speed with the largest RMS value approaching 800mm at 06:45. Examples of the different forms of these events are shown as the integrated displacement curve at the edge of the bridge deck in Fig. 11.

#### 4.3. Correlation of vibration at different sections

One interesting observation is made on the vibration mode of the structure. The structure was vibrating with the largest amplitude at Section *I* and the three sections *F*, *H* and *I* were in phase in

Fig. 14 Parameters of forced excitation response at Section *F*

the first torsional mode. But at 02:36, Section *I* moved faster by  $90^\circ$  in three cycles leading Sections *F* and *H* by  $90^\circ$ . The modal frequency remained the same before and after this change. This state remained unchanged until 07:04 when Section *I* lagged behind  $90^\circ$  in three cycles, and the three sections are in phase again. This occurrence could not be explained from inspection of existing wind and acceleration data.

A technique different from that used for typhoon BABS is adopted here to study the correlation of vibration. The correlation coefficients are computed between the time histories of the integrated displacement at Sections *F*, *H* and *I* for the periods of forced response events identified at Section *I*, and they are plotted against the amplitude of vibration and turbulence intensity in Fig. 12. Vibration at the first torsional modal frequency was observed in all these Sections. Strong correlation exists

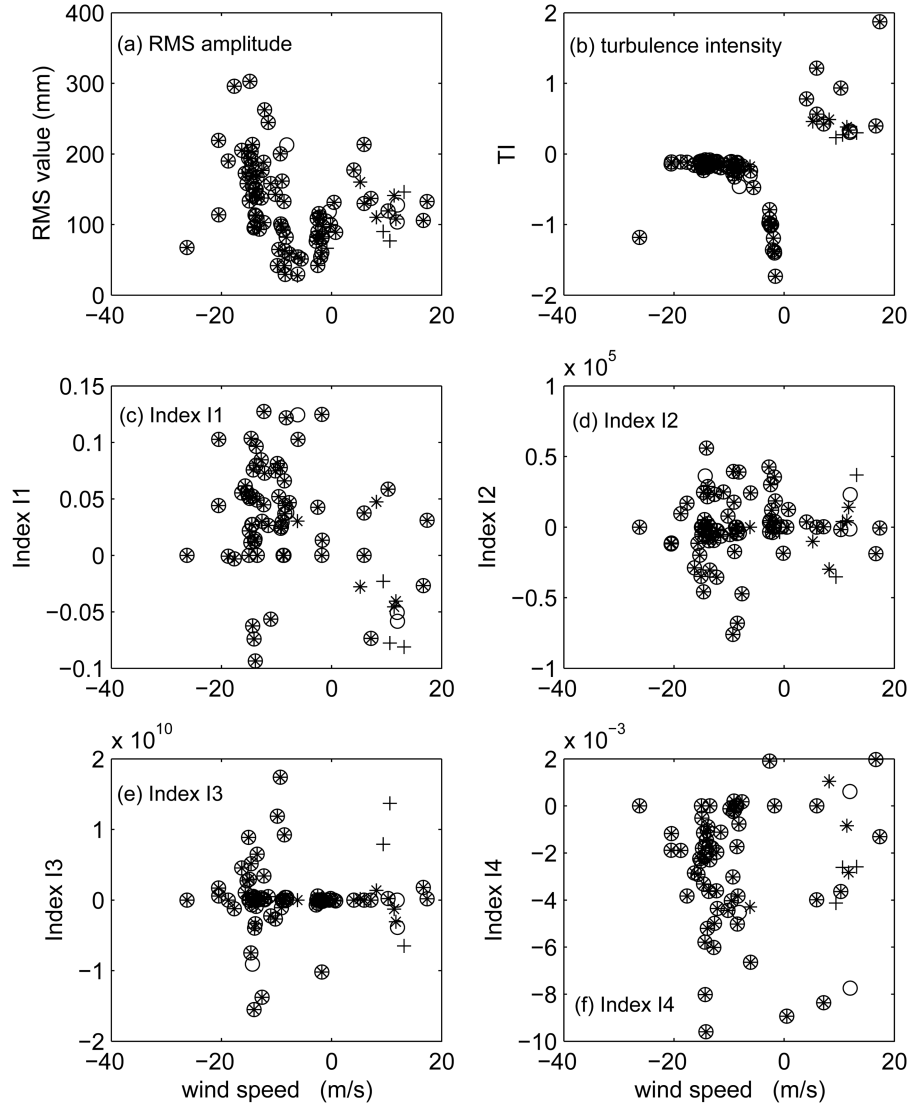


Fig. 15 Parameters of forced excitation response at Section *H* at first torsional mode (Sept. 1999)

between vibrations at Sections *F* and *H* and between *H* and *I* with values larger than 0.9 and 0.8 respectively when the RMS amplitude is greater than 200mm. The correlation between Sections *F* and *I* is weak but it increases with increasing amplitude of vibration beyond 250 mm. The turbulence intensity and vertical angle of incidence show little relationship with the correlation.

#### 4.4. Results and discussions

The RMS amplitude of vibration, the turbulence intensity and the four aerodynamic parameters given in Eq. (15) of Law, *et al.*(2007) are plotted in Figs. 13 to 16 for Sections *B*, *F*, *H* and *I* respectively.

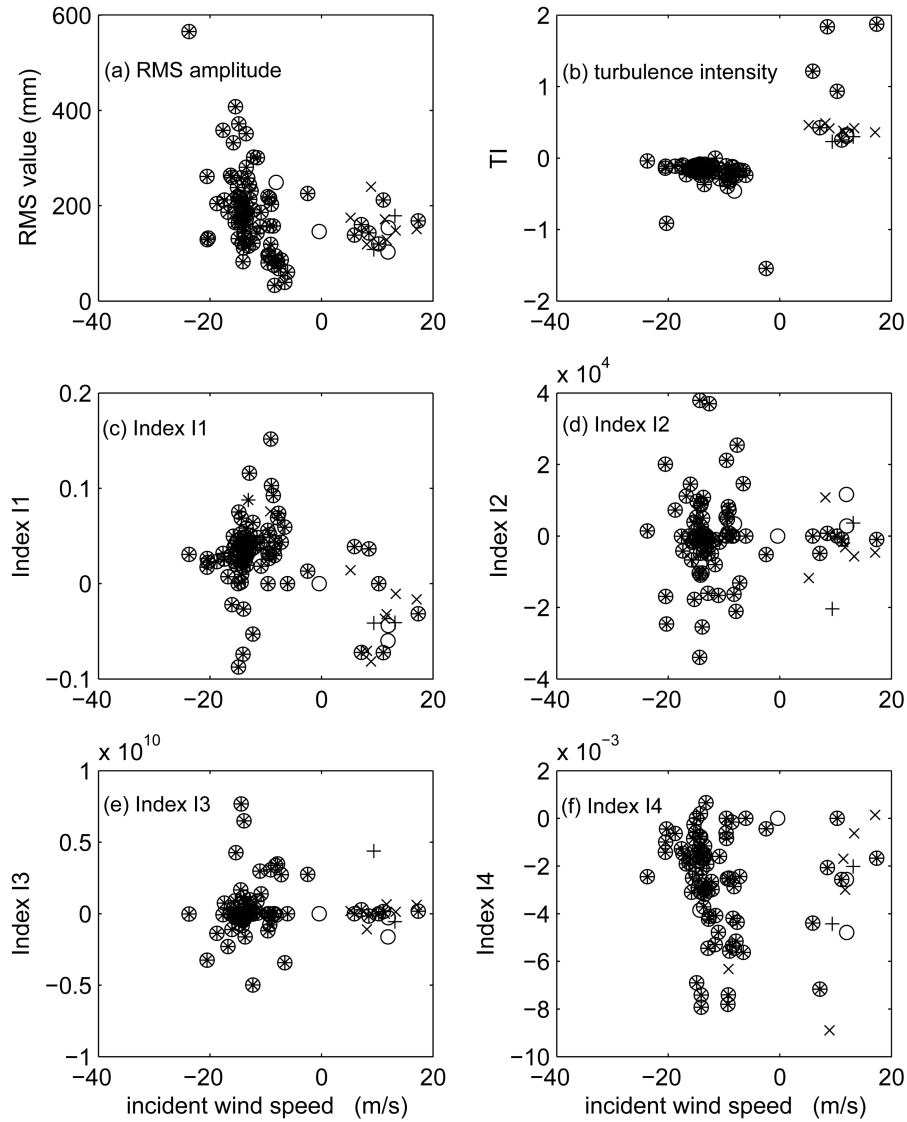


Fig. 16 Parameters of forced excitation responses at Section *I* at first torsional mode (Sept. 1999)

All the RMS amplitude plots show a distinct peak distribution of the responses at an approximate average wind speed of 16 m/s. The turbulence intensity at this wind speed is smaller than 0.3 and the parameters  $I_1$  to  $I_4$  vary with a narrow range, and they are shown in Table 1. These ranges are wider at Section *F* compared with those at Section *I*. Inspection on these results lead to the following discussions:

- Almost all the events in the group with the larger RMS values peak are associated with a vertical angle of incidence larger than  $+10^\circ$  or smaller than  $-10^\circ$  with a turbulence intensity less than 0.3 which is quite high. The critical wind speed is approximately 16.0 m/s which is within the range of 12.2 to 19.9 m/s as observed from the wind tunnel tests.
- Parameters  $I_2$  and  $I_3$  do exist in the cases studied with a range. This is expected as the strength



of wind in this typhoon is much larger than that in the second study, and non-linear aerodynamic effects exist in the large amplitude of vibration of the structure.

- Parameter  $I_4$  is mainly negative and of the same order at different sections indicating little change over a long distance. This means a very good correlation in the aerodynamic stiffness force on the structure.
- Parameter  $I_1$  takes up both positive and negative values and is of the same order at different Sections. The average of the group of data at Section  $H$  is slightly larger than that for Section  $I$ . This observation matches that in the Second Study with typhoon BABS where  $I_1$  in Section  $H$  is larger than that at Section  $I$ .

## 5. Aerodynamic effects on the bridge deck

The parameters  $I_1$  to  $I_4$  from the second and third studies have been listed in Table 1. They are related to the aerodynamic forces on the bridge deck as shown in Eqs. (4) and (15) of Law, *et al.*(2007). These forces are further calculated as ratios of the aerodynamic forces to the corresponding force of the original system in Eqs. (4) and (6), and they are shown in the last two columns of the Table. The instantaneous wind speed  $U$  is taken as the critical wind speed in calculating these ratios.

The linear damping force varies with a negative range in the second study and it has either positive or negative values in the third study. These results indicate the wind effect does exhibit negative damping under severe typhoon conditions with large vertical angle of incidence, while typhoon with a small vertical wind incidence angle exhibits only positive damping.

The linear stiffness force varies predominantly with a negative range for all the cases under study. It does have some positive values up to 4.5% at Sections  $B$  and  $I$  which are at the end pier of the West side span and the midspan of the main span respectively. This non-negative stiffness induced by typhoon YORK is relatively small. Since the events last for a short duration, it is considered not to have any significant effect on the structure.

It should be noted that this study in terms of the stiffness and damping forces of the original

Table 3 Vortex shedding events for first bending mode at section  $F$

Duration (sec.)	RMS amplitude (mm)	Velocity (m/s)	Turbulence intensity	Horizontal angle (o)	Vertical incident angle (o)	Index $I_1$	Index $I_4$
128.9	16.4	5.3	0.14	347.8	8.1	-0.105245	-0.009720
82.0	19.6	5.7	0.18	335.9	13.2	-0.021762	-0.000306
132.8	17.9	6.0	0.18	354.7	7.1	-0.024055	0.001790
105.5	15.6	6.5	0.11	197.4	1.0	-0.022942	-0.000518
109.4	14.7	7.3	0.07	135.3	-0.8	-0.026041	-0.000519
74.2	18.8	6.4	0.17	143.2	-7.4	-0.000552	0.002489
82.0	19.7	6.6	0.12	165.6	-2.8	-0.064055	0.000152
82.0	19.5	7.2	0.08	262.1	-13.2	-0.057128	-0.001451
97.7	17.5	7.0	0.16	269.6	-4.7	-0.013537	0.002700
82.0	21.0	6.1	0.20	37.8	-20.8	-0.001205	0.000010

system when modelled as a SDOF system is not conclusive. But it does give the approximate contribution of wind effect to the overall dynamics of the combined system.

## 6. Conclusions

Vortex shedding does exist in the suspension bridge Bridge in both the first torsional and second vertical modes of vibration of the structure. They are the forced responses under the wind action at mainly a single modal frequency occurring when the wind action is acting close to the critical wind speed from wind tunnel tests. Parameters related to the lifting force in a vortex shedding event are estimated through data processing on the measured wind and acceleration responses, and the subsequent analyses with a SDOF model for the event. The correlation of vibration in different sections of the bridge deck is studied, and the spatial correlation along the span is roughly proportional to the amplitude of vibration. Other major findings are:

- The RMS amplitude of vibration from field measurement is of the same order as from wind tunnel test, but vortex shedding events with a negative vertical angle of incidence gives larger amplitude of vibration than those with a positive angle. This is contrary to the observations from the wind tunnel test. Events with an angle of incidence beyond  $\pm 10^\circ$  could occur at a higher wind speed.
- Non-linear damping forces do not exist when the vertical angle of incidence is between  $\pm 5^\circ$ . However they occur with either positive or negative values when the angle of incidence is beyond  $\pm 10^\circ$ .
- The aerodynamic stiffness force is predominantly negative and the values found for all the four sections under study are similar indicating a highly correlated event along the bridge deck. The isolated events with a positive force last for short duration, and they are small with a maximum of 4.5% of the stiffness of the original system.
- The linear aerodynamic damping force is negative when the angle of incidence is between  $\pm 5^\circ$ , and it may take up either large positive or negative values when the angle is beyond  $\pm 10^\circ$ .

## Acknowledgements

The work described in this paper was supported by a grant from the Hong Kong Polytechnic University Research Funding Project No. G-S571.

## References

- Christensen, C.F. and Roberts, J.B. (1998), "Parametric identification of vortex-induced vibration of a circular cylinder from measured data", *J. Sound Vib.*, **211**(4), 617-636.
- Law, S.S., Yang, Q.S and Fang, Y.L. (2007), "Experimental studies on possible vortex shedding in the suspension bridge. Part I – Structural dynamic characteristics and analysis model", *Wind Struct.*, **10**(6), 543-554.
- Petrovski, J. and Naumovski, N. (1979), "Processing of strong motion accelerograms. Part 1: Analytical methods", Report 66. I211S, Stronjze.